

# $\bar{D}N$ interaction from meson-exchange and quark-gluon dynamics

J. Haidenbauer<sup>1</sup>, G. Krein<sup>2</sup>, Ulf-G. Meißner<sup>1,3</sup>, and A. Sibirtsev<sup>3</sup>

<sup>1</sup> Forschungszentrum Jülich, Institut für Kernphysik, D-52425 Jülich, Germany

<sup>2</sup> Instituto de Física Teórica, Universidade Estadual Paulista, Rua Pamplona, 145 - 01405-900 São Paulo, SP, Brazil

<sup>3</sup> Helmholtz-Institut für Strahlen- und Kernphysik (Theorie), Universität Bonn, Nußallee 14-16, D-53115 Bonn, Germany

Received: date / Revised version: date

**Abstract.** We investigate the  $\bar{D}N$  interaction at low energies using a meson-exchange model supplemented with a short-distance contribution from one-gluon-exchange. The model is developed in close analogy to the meson-exchange  $KN$  interaction of the Jülich group utilizing SU(4) symmetry constraints. The main ingredients of the interaction are provided by vector meson ( $\rho$ ,  $\omega$ ) exchange and higher-order box diagrams involving  $\bar{D}^*N$ ,  $\bar{D}\Delta$ , and  $D^*\Delta$  intermediate states. The short range part is assumed to receive additional contributions from genuine quark-gluon processes. The predicted cross sections for  $\bar{D}N$  for excess energies up to 150 MeV are of the same order of magnitude as those for  $KN$  but with average values of around 20 mb, roughly a factor two larger than for the latter system. It is found that the  $\omega$ -exchange plays a very important role. Its interference pattern with the  $\rho$ -exchange, which is basically fixed by the assumed SU(4) symmetry, clearly determines the qualitative features of the  $\bar{D}N$  interaction – very similar to what happens also for the  $KN$  system.

**PACS.** 14.40.Lb Charmed mesons – 12.39.Pn Potential models – 12.40.-y Other models for strong interactions – 13.75.Jz Kaon-baryon interactions

## 1 Introduction

The study of the interactions of charmed hadrons with nucleons is of interest in several contexts. One example is in experiments of relativistic heavy ion collisions (RHIC). Since long time [1] the suppression of  $J/\Psi$  production in RHIC is being considered as a possible signature for the formation of a quark-gluon plasma (QGP). The alleged suppression would occur because the deconfined quarks of the QGP screen the long range confining potential thus making impossible the formation of the mesonic bound states. However, collisions of the charmed mesons with hadrons in the medium can also lead to dissociation of these mesons, subverting therefore the screening scenario. Moreover, more recently it has been argued that heavy quarkonia could be re-formed via rescattering processes of open-charm hadrons in the late stages of RHIC which would then lead to an enhanced  $J/\Psi$  production [2]. Thus, it seems clear that a good knowledge of the interaction of charmed mesons with ordinary hadrons like nucleons is a prerequisite for differentiating between these scenarios. For a recent review on these issues, see Ref. [3]. Another example where the interaction of charmed mesons with ordinary hadrons is of interest refers to studies of chiral symmetry restoration in a hot and/or dense medium. In this respect, the interaction of charmed  $D$  mesons - which are composed of one light and one heavy quark - with nucleons is of particular interest. The properties of the

light quarks in a  $D$  meson are sensitive to temperature and density and, therefore, changes in the properties of the  $D$  mesons in medium can be expected. Consequently, one can also expect that their interactions with nucleons will change in the medium. The  $D$  meson and its lowest excitations are somewhat special in this respect because their spectroscopy is simpler than of ordinary mesons composed solely by  $u$  and  $d$  quarks. This is so because the charm quark  $c$  is much heavier than the light  $u$  and  $d$  quarks, and to a good approximation these mesons can be described as one-body bound states, a fact that simplifies tremendously their study.

Before one can infer in a sensible way changes of the interaction in the medium, a reasonable understanding of the interaction in free space is required. However, here one has to cope with a major difficulty, namely the complete lack of experimental data at low energies for the free-space interaction. This situation is hopefully going to change soon with the operation of the FAIR facility at the GSI laboratory in Germany. There are proposals for experiments by the PANDA collaboration [4] at this facility to produce  $D$  mesons by annihilating antiprotons on the deuteron and, through the rescattering of the produced  $D$  and  $\bar{D}$  mesons on the spectator nucleon [5], to determine  $DN$  as well as  $\bar{D}N$  cross sections and possibly even phase shifts. Still, for the design of detectors and of efficient data acquisition systems, estimates for the magnitude of such cross sections are urgently required. Therefore, there is a

need for developing models of the interaction of charmed particles with ordinary hadrons, and since – as said – not much is known empirically, such models can only and should be constrained as much as possible by symmetry arguments, analogies with other similar processes, and the use of different degrees of freedom.

The interaction of charmed mesons with ordinary hadrons composed of  $u$  and  $d$  quarks has been investigated using effective hadronic Lagrangians and quark models. Most of the studies have concentrated on the interaction of  $J/\psi$  and other heavy charmonia with ordinary hadrons, mainly due to the interest in the QGP suppression hypothesis alluded above – see Ref. [6] for a review on these investigations. With respect to the interaction of the  $D$  meson with the nucleon, which is the subject of the present paper, not much is known. The work of Ref. [7], using an effective SU(4) hadronic Lagrangian, to the best of our knowledge was the first one to provide estimates of cross sections for the  $DN$  system in Born approximation. In terms of quark degrees of freedom, the authors of Ref. [8] have made an estimate for the  $DN$  cross sections using quark rearrangement arguments and concluded that such cross sections should be equal to the corresponding  $KN$  cross sections, though no explicit model was employed. (See also the results presented in Ref. [9]).

In the present paper we investigate the  $\bar{D}N$  interaction within a meson-exchange model and a quark model utilizing one-gluon-exchange (OGE), in the spirit of a recent study of the  $KN$  system by us [10]. ( $\bar{D}$  is used here generically for the  $\bar{D}^0$  and  $D^-$  isospin doublet which contains a  $\bar{c}$  quark, and corresponds to  $K$  consisting of the  $K^+$  and  $K^0$  isospin doublet with an  $\bar{s}$  quark.) To be more specific, the  $\bar{D}N$  interaction we construct is an extension of the  $KN$  meson-exchange model of the Jülich group [11, 12, 13], generalized by assuming as a working hypothesis SU(4) symmetry constraints. Note that the  $KN$  model described in Refs. [11, 12] considered not only single boson exchanges ( $\sigma$ ,  $\rho$ ,  $\omega$ ), but also contributions from higher-order diagrams involving  $N$ ,  $\Delta$ ,  $K$  and  $K^*$  intermediate states. We focus on the  $\bar{D}N$  system because it has the advantage that its dynamics should be governed predominantly by the same “long-range” physics as the  $KN$  interaction, i.e. by the exchange of ordinary (vector and possibly scalar) mesons. Thus, fairly reliable and, most importantly, essentially parameter-free predictions can be made once one accepts the constraints provided by SU(4) symmetry. The  $DN$  system is expected to exhibit a much richer structure [14] and thus may be more interesting [15, 16, 17], but it involves also much larger uncertainties. In this case, like in the analogous  $\bar{K}N$  system, there are couplings to several other channels which are already open near the  $DN$  threshold ( $\Lambda_c\pi$ ,  $\Sigma_c\pi$ ) or open not far from the threshold ( $\Lambda_c\eta$ ). It is obvious that the coupling to those channels must play a crucial role for the dynamics of the  $DN$  system – as it does in the corresponding  $\bar{K}N$  system – and, thus, will have a strong impact on any quantitative results. But the transitions to those channels and the interactions in those channels involve charmed baryon resonances as well as the exchange of charmed mesons, for example the

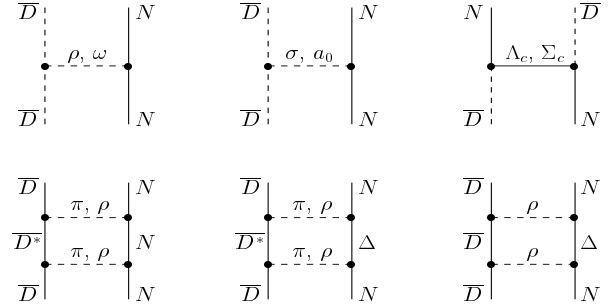


**Fig. 1.** Meson-exchange contributions included in the  $\bar{D}N$  interaction.

$D^*(2010)$ , whose coupling constants and associated vertex form factors, required in any meson-exchange model, are practically unknown and difficult to constrain.

Our  $\bar{D}N$  model is obtained by substituting the one-boson-exchange contributions, but also the box diagrams involving  $K^*N$ ,  $K\Delta$ , and  $K^*\Delta$  intermediate states, of the original  $KN$  model of the Jülich group by the corresponding contributions to the  $\bar{D}N$  interaction under the constraint of SU(4) symmetry. Regarding the short-ranged quark part, we use the dominant contributions of OGE exchange, which are the Coulomb and spin-spin parts. These are of the same form as for the  $KN$  interaction, but the mass of the charm quark is much heavier than the one of the strange quark, and the size parameter of the meson wave function is also different. Therefore, the  $\bar{D}N$  interaction will be different from the  $KN$  interaction. We want to emphasize that we iterate the effective meson-exchange and OGE potentials in a Lippmann-Schwinger equation, contrary to the common practice of using only Born approximation [7, 8, 9]. We found that the effect of iteration on the predicted cross sections can be quite substantial, being of the order of 50 % in some cases.

The plan of our paper is the following. In the next section we specify the three-meson vertices used in the paper. Specifically, we discuss the constraints of SU(4) symmetry to relate the required new couplings and present the numerical values of vertex parameters. The interaction Lagrangians, which are needed to complete the derivation of the meson-baryon potential, are presented in Appendix A. In Section 3 we discuss the quark-gluon exchange mechanism for the  $\bar{D}N$  interaction. The detailed derivation of the equations shown in this Section are outlined in Appendix B. Our numerical results are presented in Section 4. The paper ends with a short summary.

## 2 The $\bar{D}N$ interaction in the meson-exchange picture

The meson-exchange model of the  $\bar{D}N$  interaction is constructed in close analogy to the corresponding  $KN$  potentials developed by the Jülich group some time ago [11, 12].

In those models, derived within time-ordered perturbation theory, not only single-meson (and baryon) exchanges were taken into account, but also higher-order box diagrams involving  $K^*N$ ,  $K\Delta$ , and  $K^*\Delta$  intermediate states. Thus, we will consider the corresponding contributions to the  $\bar{D}N$  interaction too, cf. Fig. 1. The general scheme and also the explicit expressions for the various contributions to the interaction potential are described in detail in Refs. [11,12] and, therefore, we do not reproduce them in the present paper. We only summarize the used interaction Lagrangians in Appendix A. Here we want to focus on the  $SU(4)$  structure which is used to extend and relate the  $\bar{D}N$  interaction to the  $KN$  system.

For the construction of the  $\bar{D}N$  interaction we need three-meson vertices involving charmed mesons of the kind  $PPV$  and  $VVP$  ( $P$  = pseudoscalar meson,  $V$  = vector meson). The general form of the  $SU(4)$  invariant Lagrangian is

$$\begin{aligned} \mathcal{L}_{MMM} = & g_{\{15\}}[-\alpha \text{Tr}(\{M_{\{15\}}, M_{\{15\}}\}M_{\{15\}}) \\ & + (1-\alpha)\text{Tr}(\{M_{\{15\}}, M_{\{15\}}\}M_{\{15\}})] \\ & + g_{\{15\}\{15\}\{1\}}(1-\alpha)\text{Tr}(\{M_{\{15\}}, M_{\{15\}}\}M_{\{1\}}) \\ & + g_{\{15\}\{1\}\{15\}}(1-\alpha)\text{Tr}(\{M_{\{15\}}, M_{\{1\}}\}M_{\{15\}}) \\ & + g_{\{1\}}(1-\alpha)\text{Tr}(\{M_{\{1\}}, M_{\{1\}}\}M_{\{1\}}), \end{aligned} \quad (1)$$

where  $\alpha$  is the  $F/(F+D)$  ratio and  $M_{\{15\}}$  ( $M_{\{1\}}$ ) stands for the  $SU(4)$  meson-15-plet (-singlet) matrix. For pseudoscalar ( $P$ ) and vector ( $V$ ) mesons  $M_{\{15\}}$  are  $4 \times 4$  matrices which are given in Table 1. Note that the  $PPV$  vertices involve only  $F$ -type coupling ( $\alpha = 1$ ) if we require charge conjugation invariance while the  $VVP$  vertices involve only  $D$ -type coupling ( $\alpha = 0$ ). Let us stress again that  $SU(4)$  should not be a flavor symmetry of QCD but rather a working hypothesis to get a handle on the various couplings and form factors employed in our model. It is, of course, strongly broken due to the use of the very different physical masses of the various mesons.

Based on the assumed  $SU(4)$  symmetry all relevant three-meson coupling constants can be derived from the empirically known  $\pi\pi\rho$  coupling. In the Jülich model [12] the value  $g_{\pi\pi\rho} = 6.0$  is used. The coupling constants of the other vertices that follow from this value are listed in Table 2.

As far as the coupling constants belonging to the  $NN$  and  $N\Delta$  vertices are concerned we take precisely the same values as in Ref. [12], which are based on those of the (full) Bonn  $NN$  potential, cf. Ref. [18]. These coupling constants are listed in Table 2 too. The Jülich  $KN$  potential contains also vertex form factors  $F$  that are meant to take into account the extended hadron structure and are parametrized in the conventional monopole or dipole form [11,12]. In the present study of the  $\bar{D}N$  system the cut-off masses appearing in those form factors for the various three-meson and baryon-baryon-meson vertices are likewise taken over from Ref. [12]. Specifically, we make the assumption that  $F_{\bar{D}\bar{D}m}(\mathbf{q}_m^2) \simeq F_{KKm}(\mathbf{q}_m^2)$ . This prescription is motivated by the notion that those form factors parametrize predominantly the off-mass-shell behaviour

of the exchanged particles – which are indeed the same in the  $KN$  and in the  $\bar{D}N$  interaction.

Let us make some more comments about the coupling constants at the three-meson vertices.  $SU(4)$  symmetry implies the following for the vector meson coupling constants relevant for our study:

$$\begin{aligned} g_{KK\omega_8} &= \sqrt{3}g_{KK\rho} = \sqrt{3}\frac{1}{2}g_{\pi\pi\rho}, \quad g_{KK\omega_{15}} = 0 \\ g_{\bar{D}\bar{D}\omega_8} &= \sqrt{\frac{1}{3}}g_{KK\rho}, \quad g_{\bar{D}\bar{D}\omega_{15}} = \sqrt{\frac{8}{3}}g_{KK\rho} \end{aligned} \quad (2)$$

$$g_{\bar{D}\bar{D}\rho} = g_{KK\rho} = \frac{g_{\pi\pi\rho}}{2}. \quad (3)$$

Assuming ideal mixing of the  $\omega_{15}$ ,  $\omega_8$  and  $\omega_1$  one obtains for the coupling constants of the physical  $\omega$  and  $\phi$

$$\begin{aligned} g_{\bar{D}\bar{D}\omega} &= \sqrt{\frac{1}{2}}g_{\bar{D}\bar{D}\omega_1} + \sqrt{\frac{1}{3}}g_{\bar{D}\bar{D}\omega_8} + \sqrt{\frac{1}{6}}g_{\bar{D}\bar{D}\omega_{15}} \\ g_{\bar{D}\bar{D}\phi} &= -\sqrt{\frac{1}{4}}g_{\bar{D}\bar{D}\omega_1} + \sqrt{\frac{2}{3}}g_{\bar{D}\bar{D}\omega_8} - \sqrt{\frac{1}{12}}g_{\bar{D}\bar{D}\omega_{15}}. \end{aligned} \quad (4)$$

The same relation holds also for the  $K$  meson. In case of the  $K$  meson the coupling constant  $g_{KK\omega}$  is given by that of  $g_{KK\omega_8}$  alone, since there is no singlet coupling for  $PPV$  vertices as mentioned above:

$$g_{KK\omega} = \sqrt{\frac{1}{3}}g_{KK\omega_8} = g_{KK\rho}. \quad (5)$$

This is the coupling constant used in the Jülich  $KN$  models [11,12]. In case of the  $D$  meson the coupling constant is given by

$$g_{\bar{D}\bar{D}\omega} = \sqrt{\frac{1}{3}}g_{\bar{D}\bar{D}\omega_8} + \sqrt{\frac{1}{6}}g_{\bar{D}\bar{D}\omega_{15}} = g_{KK\rho}. \quad (6)$$

Summarizing the above results from Eqs. (3,5,6) we see that

$$\begin{aligned} g_{\bar{D}\bar{D}\rho} &= g_{KK\rho} \\ g_{\bar{D}\bar{D}\omega} &= g_{KK\omega}. \end{aligned} \quad (7)$$

Thus, the coupling constants of the exchanged vector mesons are the same for the  $KN$  and  $\bar{D}N$  systems under assumption of  $SU(4)$  symmetry and ideal mixing.

Since some of the couplings involving the  $D$  meson are known empirically, at least to some extent, we want to review them briefly here. The  $DD\rho$  coupling constant was determined in Refs. [19,20] based on the vector dominance model and found to be  $g_{DD\rho} = 2.52 - 2.8$ . This value, which was subsequently adopted in several investigations [7,21,22], is only marginally smaller than the one which follows from assuming  $SU(4)$  symmetry. The same is true for the  $DD\omega$  coupling constant, found to be  $g_{DD\omega} = -2.84$  in Ref. [20], likewise derived within the vector dominance model. In Ref. [22] the value  $g_{\pi DD^*} = 5.56$  is cited, derived from the measured decay width of the  $D^*$

**Table 1.** SU(4) matrix representation of the pseudo-scalar ( $P$ ) and vector ( $V$ ) mesons.

$$P = \begin{pmatrix} \frac{\pi^0}{\sqrt{2}} + \frac{\eta}{\sqrt{6}} + \frac{\eta_c}{\sqrt{12}} & \pi^+ & K^+ & \bar{D}^0 \\ \pi^- & -\frac{\pi^0}{\sqrt{2}} + \frac{\eta}{\sqrt{6}} + \frac{\eta_c}{\sqrt{12}} & K^0 & D^- \\ K^- & \bar{K}^0 & -\sqrt{\frac{2}{3}}\eta + \frac{\eta_c}{\sqrt{12}} & D_s^- \\ D^0 & D^+ & D_s^+ & -\frac{3\eta_c}{\sqrt{12}} \end{pmatrix}$$

$$V = \begin{pmatrix} \frac{\rho^0}{\sqrt{2}} + \frac{\omega_8}{\sqrt{6}} + \frac{\omega_{15}}{\sqrt{12}} & \rho^+ & K^{*+} & \bar{D}^{*0} \\ \rho^- & -\frac{\rho^0}{\sqrt{2}} + \frac{\omega_8}{\sqrt{6}} + \frac{\omega_{15}}{\sqrt{12}} & K^{*0} & D^{*-} \\ K^{*-} & \bar{K}^{*0} & -\sqrt{\frac{2}{3}}\omega_8 + \frac{\omega_{15}}{\sqrt{12}} & D_s^{*-} \\ D^{*0} & D^{*+} & D_s^{*+} & -\frac{3\omega_{15}}{\sqrt{12}} \end{pmatrix}$$

**Table 2.** Vertex parameters used in the meson-exchange model of the  $\bar{D}N$  interaction at the  $\bar{D}\bar{D}m_r$  or  $\bar{D}\bar{D}^*m_r$  (M) and  $NNm_r$  or  $N\Delta m_r$  (B) vertices.  $M_r$  and  $m_r$  refers to the mass of the exchanged particle. Note that the scalar meson exchanges ( $\sigma$ ,  $a_0$ ) are considered as an effective interaction, cf. text, and therefore we provide only the product of the coupling constants.

Process	Exch. part.	$M_r$ or $m_r$ [MeV]	$g_M/\sqrt{4\pi}$	$g_B/\sqrt{4\pi}$ [ $f_B/g_B$ ]	$\Lambda_M$ [GeV]	$\Lambda_B$ [GeV]
$\bar{D}N \rightarrow \bar{D}N$	$\rho$	769	0.843	0.917 [6.1]	1.4	1.6
	$\omega$	782.6	0.843	2.750 [0.0]	1.5	1.5
	$\Lambda_c$	2285	-2.284	-2.284	4.1	4.1
	$\Sigma_c$	2455	0.435	0.435	4.1	4.1
	$\sigma$	600		0.25 (1.00)	1.7	1.2
	$a_0$	980		0.65 (2.60)	1.5	1.5
$\bar{D}N \rightarrow \bar{D}^*N$	$\pi$	138.03	0.843	3.795	1.3	0.8
$\bar{D}N \rightarrow \bar{D}^*\Delta$	$\rho$	769	0.843	0.917 [6.1]	1.4	1.0
	$\pi$	138.03	0.843	0.600	1.2	0.8
$\bar{D}N \rightarrow \bar{D}\Delta$	$\rho$	769	0.843	5.740	1.3	1.0
	$\rho$	769	0.843	5.470	1.3	1.6

meson. Here the corresponding SU(4) coupling constant is roughly a factor 2 smaller.

In any case, in our model calculation we use coupling constants that are determined fully by SU(4) symmetry. The difference to those values deduced from available experimental information is not very large and, thus, does not really warrant a departure from SU(4) at present. Indeed, there are other assumptions made in the model calculation, that could be considered to be more questionable, for example those about the vertex form factor. As mentioned above, the prescription we use relies on the fact that the same particles are exchanged in the  $KN$  and  $\bar{D}N$  potentials. Possible influences from differences in the off-mass-shell dependence due to the different ( $KN$  or  $\bar{D}N$ ) intermediate states, appearing in higher iterations, are simply ignored. However, the main uncertainty in the meson-exchange model arises from the treatment of the scalar-meson sector. Here, unlike for pseudoscalar and vector mesons, so far there is no general agreement about who are the actual members of the lowest lying scalar-meson SU(3) multiplet. (For a thorough discussion on that issue and an overview of the extensive literature we refer the reader to [23,24] and references therein.) Therefore, it remains unclear whether and how the relations for the

coupling constants given in Eq. (1) should be applied in the SU(3) case [12,25], but even more so when it comes to SU(4). It is known for a long time that the contributions from the scalar sector play a crucial role in any baryon-baryon and meson-baryon interaction at intermediate ranges.

In the present paper we consider two different scenarios for the scalar mesons. First, in line with the works in Refs. [12,25], we view the contributions in the scalar sector as being due to correlated  $\pi\pi$  and  $K\bar{K}$  exchange. However, in the absence of a concrete model for those contributions, as it was used in [12,25], we resort here to a rough estimation of their strength. Based on the scale of the correlated  $\pi\pi$  and  $K\bar{K}$  exchange, which we identify with the masses of the relevant propagators –  $\rho$  ( $K^*$ ) and/or  $\pi\pi$  ( $K\bar{K}$ ) for the  $\pi N$  and  $KN$  interactions, but the  $D^*(2010)$  and/or  $\bar{D}D$  for the  $\bar{D}N$  system – we expect that its strength should be about 4 times smaller in the latter case. Thus, we reduce the coupling constants by that factor as compared to the values used in [10]. Note that this reduction is supported by available model calculations of the reaction  $p\bar{p} \rightarrow D\bar{D}$  [26,27] which suggest that the corresponding amplitude, which would form the main ingredient for a microscopic calculation of the cor-

related  $\pi\pi$  exchange for  $\bar{D}N$ , cf. Ref. [12], is significantly smaller than the one for  $p\bar{p} \rightarrow K\bar{K}$ , even when taking into account the kinematical differences. The used values are given in Table 2. The second scenario is an attempt to simulate the case that the scalar contributions are due to genuine scalar-meson exchange. Accordingly, we use the same scalar coupling constants for the  $\bar{D}N$  interaction as in the  $KN$  model [10]. The concrete values for that scenario are listed in brackets in Table 2.

### 3 The $\bar{D}N$ interaction based on the quark-gluon exchange mechanism

The quark interchange processes with one-gluon-exchange (OGE) we consider in the present paper are represented pictorially in Fig. 2. In these graphs, the  $D$  mesons are  $\bar{D}^0 = u\bar{c}$  and  $D^- = d\bar{c}$ , so that the exchanged quarks are always the light  $u$  and  $d$  quarks, the  $\bar{c}$  antiquarks are not interchanged. The dominant contributions of the OGE interaction are the Coulomb and spin-spin parts. The interaction of the quarks  $i$  and  $j$  with constituent masses  $m_i$  and  $m_j$  can be written as  $V_{ij} = T_i^a T_j^a V_{ij}(q, S)$ , where  $T^a = \lambda^a/2$  for a quark and  $T^a = -(\lambda^a)^T/2$  for an antiquark, and the momentum and spin dependent pieces as  $V_{ij}(q, S)$  are given as

$$\begin{aligned} V_{ij}(q, S) &= v_C(q) + v_{SS}(q) \mathbf{S}_i \cdot \mathbf{S}_j \\ &= \frac{4\pi\alpha_s}{q^2} - \frac{8\pi\alpha_s}{3m_i m_j} \mathbf{S}_i \cdot \mathbf{S}_j, \end{aligned} \quad (8)$$

where  $\alpha_s$  is the quark-gluon coupling constant.

As shown in more detail in Appendix B, the effective  $\bar{D}N$  potential  $\mathcal{V}_{\bar{D}N}$  can be written as a sum of four contributions as

$$\mathcal{V}_{\bar{D}N}(\mathbf{p}, \mathbf{p}') = \sum_{i=1}^4 \omega_i [V_i(\mathbf{p}, \mathbf{p}') + V_i(\mathbf{p}', \mathbf{p})] / 2, \quad (9)$$

where each term in the sum corresponds to a graph in Fig. 2. The  $\omega_i$ 's are given Table 3; they come from summing over the color-flavor-spin indices of the quarks and include symmetry combinatorial factors. The  $V_i$ 's are functions of the center-of-mass momenta  $\mathbf{p}$  and  $\mathbf{p}'$  which are given by multidimensional overlap integrals over the internal wave functions of the nucleons and mesons and the OGE potentials. When using Gaussian forms for the nucleon and meson wave functions, many of the integrals can be done analytically and the  $V_i$ 's can then be expressed in terms of a single three-dimensional integral as

$$\begin{aligned} V_i(\mathbf{p}, \mathbf{p}') &= e^{-a_i p^2 - b_i p'^2 + c_i \mathbf{p} \cdot \mathbf{p}'} \left[ \frac{3g}{(3 + 2g)\pi\alpha_N^2} \right]^{3/2} \\ &\times \int \frac{d^3q}{(2\pi)^3} v(q) e^{-d_i q^2 + e_i \cdot \mathbf{q}}, \end{aligned} \quad (10)$$

where  $v(q) = v_C(q)$ , or  $v_{SS}(q)$  defined in Eq. (8),  $g = \alpha_N^2/\beta_D^2$ , where  $\alpha_N$  and  $\beta_D$  are the Gaussian widths of the nucleon and the  $D$  meson. The  $a_i, b_i, \dots$  are given in terms of  $g$  and the quark masses – see Appendix B.

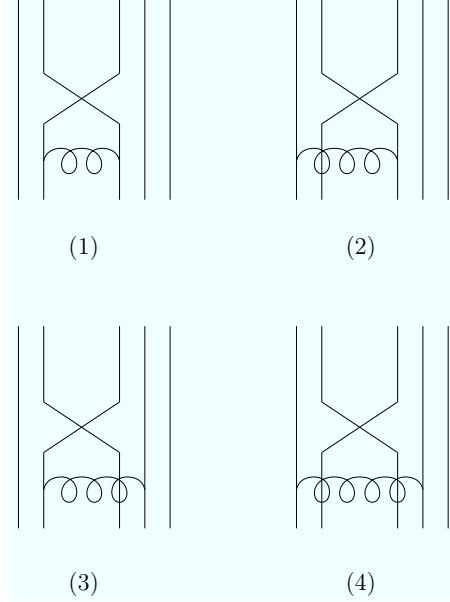


**Fig. 2.** Pictorial representation of the four different quark-interchange processes that contribute to the  $\bar{D}N$  interaction. The wavy lines represent the one-gluon exchange (OGE) and the solid lines represent quarks.

### 4 Results and discussion

The original  $KN$  model of the Jülich group includes besides the exchange of the standard mesons also an additional phenomenological (extremely short-ranged) repulsive contribution, a “ $\sigma_{rep}$ ”, with a mass of about 1.2 GeV [12]. This contribution was introduced ad-hoc in order to achieve a simultaneous description of the empirical  $KN$   $S$ - and  $P$ -wave phase shifts, but it is also required for a consistent description of the  $KN$  and  $\bar{K}N$  systems [28], which are interrelated via a  $G$ -Parity transformation. Evidently, due to its phenomenological nature it remains unclear how that contribution should be treated when going over to the  $\bar{D}N$  system. Fortunately, a recent investigation by our group provided evidence that a significant part of that short-ranged repulsion required in the original Jülich model could be due to genuine quark-gluon exchange processes. Thus, in the present study we will build upon this insight when constructing a model of the  $\bar{D}N$  interaction. In particular this means that also for the  $\bar{D}N$  system we consider contributions from meson-exchange as well as from quark-gluon mechanisms where each of them is closely linked to the corresponding pieces in the  $KN$  interaction. However, in order to get a better understanding on what changes and what remains the same in the transition from  $KN$  to  $\bar{D}N$  we will first study those sectors separately. In order to facilitate an easy comparison of the  $KN$  and  $\bar{D}N$  results we present them as a function of the corresponding excess energies. (One should be aware that a comparison at the same laboratory momentum, say, would look quite different because of the large mass difference between the kaon and the  $D$  meson.) Within the range shown the  $KN$  and  $\bar{D}N$  reactions are predominantly elastic. The

**Table 3.** The color-spin-flavor coefficients from the spin-spin OGE interaction for the  $\omega_i$  for the  $D^-N$  and  $\bar{D}^0N$  systems for the individual charge states, and for the  $I = 0$  and  $I = 1$  combined isospin states.

Process	$\omega_1$		$\omega_2$		$\omega_3$		$\omega_4$	
	$1_i 1_j$	$S_i S_j$	$1_i 1_j$	$S_i S_j$	$1_i 1_j$	$S_i S_j$	$1_i 1_j$	$S_i S_j$
$p \bar{D}^0 \rightarrow p \bar{D}^0$	1/3	1/3	1/3	1/3	1/3	1/18	1/3	1/18
$n D^- \rightarrow n D^-$	1/3	1/3	1/3	1/3	1/3	1/18	1/3	1/18
$p D^- \rightarrow p D^-$	1/3	1/6	1/3	1/6	1/3	1/9	1/3	1/9
$n \bar{D}^0 \rightarrow n \bar{D}^0$	1/3	1/6	1/3	1/6	1/3	1/9	1/3	1/9
$p D^- \rightarrow n \bar{D}^0$	1/3	1/6	1/3	1/6	1/3	-1/18	1/3	-1/18
$I = 0$	0	0	0	0	0	-1/6	0	-1/6
$I = 1$	-4/9	-1/3	+4/9	-1/3	+4/9	-1/18	-4/9	-1/18

first inelastic hadronic channel (pion production) opens at an excess energy of around 136 MeV. We want to mention also that, due to the much smaller mass difference between  $D^*(2010)$  and  $D(1869)$  versus  $K^*(892)$  and  $K(496)$ , the nominal threshold of the  $D^*N$  channel occurs at a significantly smaller excess energy than the corresponding  $K^*N$  channel. Indeed the former practically coincides with the  $DN\pi$  threshold.

Based on the  $\bar{D}N$  interaction potential  $\mathcal{V}$  described in the two preceding sections the corresponding reaction amplitude  $\mathcal{T}$  is obtained by solving a Lippmann-Schwinger type scattering equation defined by the time-ordered perturbation theory,

$$\mathcal{T} = \mathcal{V} + \mathcal{V}\mathcal{G}_0\mathcal{T},$$

from which we calculate the  $\bar{D}N$  observables in the standard way [11]. Due to the large mass of the  $D$  meson that enters into the free Green's function  $G_0$  higher iterations play a somewhat less important role for  $\bar{D}N$  as compared to the  $KN$  system. But we want to emphasize that unitarization of the reaction amplitude, which is achieved by solving Eq. (11), is essential for obtaining meaningful results because the resulting phase shifts in the  $S$ - and also  $P$ -waves are in the order of 20 degrees or even more in the energy range covered by our study. For completeness let us also mention that we use averaged masses for the  $D$  mesons, namely  $m_D=1866.9$  MeV and  $m_{D^*}=2009$  MeV.

Results based on the meson-exchange contributions are shown in Figs. 3 (for isospin  $I = 0$ ) and 4 (for  $I = 1$ ). Since some of the  $\bar{D}N$  model calculations in the literature take into account only  $\rho$  exchange [7,9] we consider its contribution first. It is obvious that the resulting cross sections for the  $\bar{D}N$  system are much larger than those for  $KN$ . But one should keep in mind that this difference is primarily caused by the different kinematics (masses). The involved coupling constants are exactly the same for the  $KN$  and  $\bar{D}N$  interactions under the assumption of SU(4) symmetry, as discussed in Sect. 2. It is worth noting that the cross section in the  $I = 0$  channel of the  $\bar{D}N$  is particularly large and even exceeds 100 mb near threshold, while for  $I = 1$  is less than 5 mb over the whole considered energy range.

The picture changes drastically once  $\omega$  exchange is added. Specifically, in the  $I = 0$  channel its contribution interferes destructively with the (attractive)  $\rho$  exchange

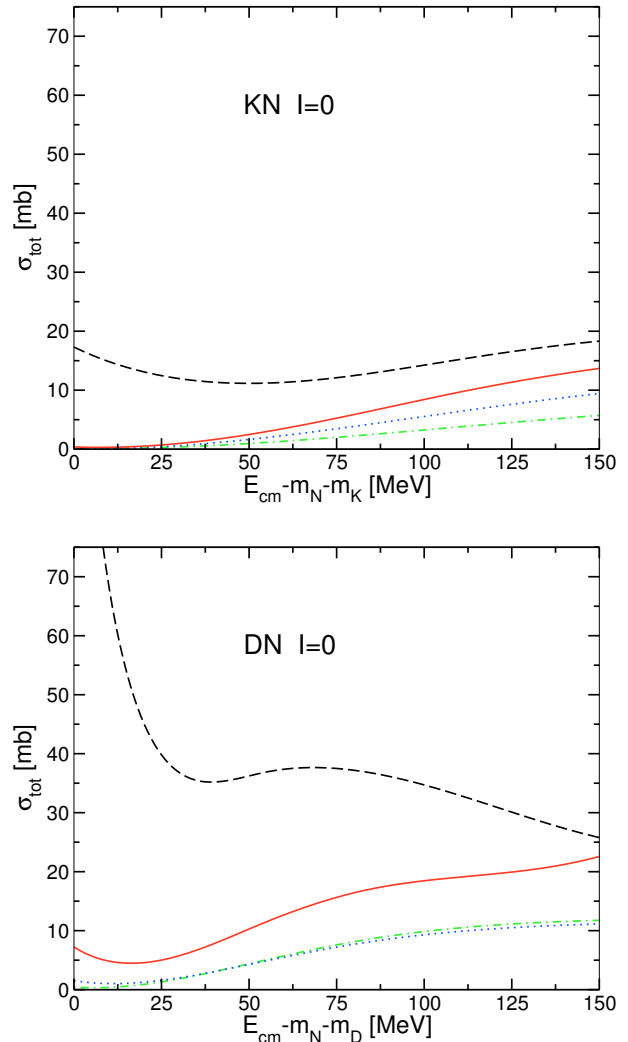


**Fig. 3.**  $KN$  and  $\bar{D}N$  cross sections in the isospin channel  $I=0$  including consecutively  $\rho$  (dashed curve),  $\omega$  (dash-dotted), scalar mesons and baryon-exchange diagrams (dotted), and box diagrams (solid).

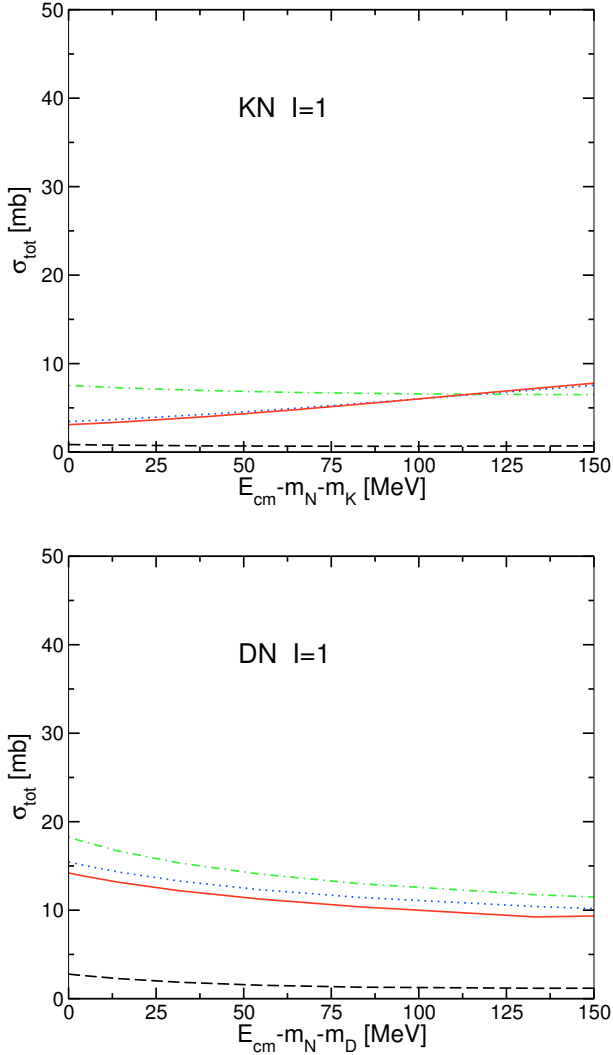


**Fig. 4.**  $KN$  and  $\bar{D}N$  cross sections in the isospin channel  $I=1$ . Same description of curves as in Fig. 3.

and leads to a strong reduction of the predicted cross section. On the other hand, for  $I = 1$  both contributions are repulsive and add up so that now the cross sections in both isospin channels are of comparable magnitude. Indeed after inclusion of the  $\omega$  exchange the  $KN$  results show already the typical features of the full model [12] but also of the experimental information [29], namely an almost constant cross section for  $I = 1$  and a cross section for  $I = 0$  that is practically zero at threshold and then increases with energy. The predictions for the  $\bar{D}N$  system exhibit very similar features.

The addition of the scalar contributions and of baryon ( $\Lambda_c(2285)$ ,  $\Sigma_c(2455)$ ) exchange influences the results for  $\bar{D}N$  very little and therefore we don't show them separately. This is not too surprising in view of our assumption about the origin of the scalar sector (we will come back to this issue later) and of the large mass of the exchanged baryons. On the other hand, the box diagrams yield a sizeable contribution, in particular in the  $I = 0$  channel of the  $\bar{D}N$  system.

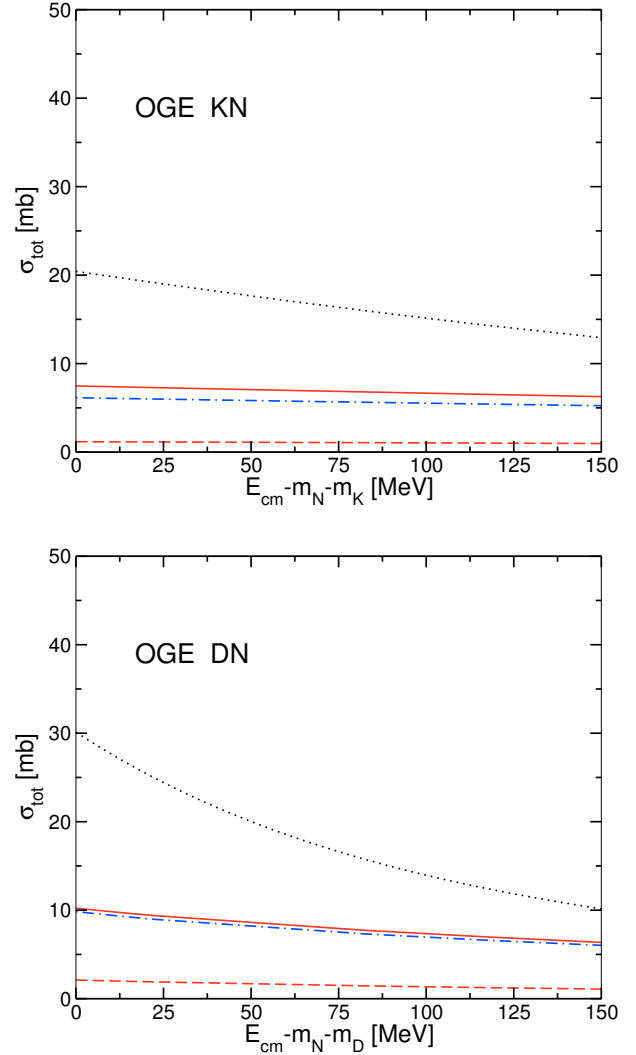


**Fig. 5.**  $KN$  and  $\bar{D}N$  cross sections from OGE. The dashed-dotted (dashed) curve is the result for the spin-spin ( $SS$ ) part in the  $I = 1$  ( $I = 0$ ) channel. The solid curve is the result for the  $I = 1$  channel after adding the Coulomb part. The dotted curve is the corresponding cross section as obtained in Born approximation. For the  $I = 0$  channel the Coulomb component is zero so that the full OGE result coincides with the curve for the  $SS$  part.

Results for the  $KN$  and  $\bar{D}N$  interactions based on the OGE in the quark model are presented in Fig. 5. We use standard quark model parameters [30]. For the light quark masses we take  $m_u = m_d = 330$  MeV and for the strange and charm quark masses we use  $m_s = 550$  MeV and  $m_c = 1600$  MeV, and the quark-gluon coupling is taken to be  $\alpha_s = 0.6$ . The size parameters of the nucleon and the kaon wave functions are  $\alpha_N = 400$  MeV and  $\beta_D = 350$  MeV. For the  $D$  meson wave function we use the value of Ref. [31], namely  $\beta_D = 383.5$  MeV. The results demonstrate that, as in the case of  $KN$ , the spin-spin component of the OGE is much more important than the Coulomb component. (Note that the contribution of the Coulomb component is zero in the  $I = 0$  channel.)

We have performed exploratory calculations utilizing a larger value for  $\beta_D$  for the  $D$  meson,  $\beta_D = 440$  MeV, as given by a recent calculation [32]. The results for the combined Coulomb and spin-spin OGE do not change appreciably, although the Coulomb part is a little smaller in this case as compared to the corresponding value with  $\beta_D = 383.5$  MeV.

The cross sections predicted for the  $\bar{D}N$  system are roughly a factor 1.5 larger than those for  $KN$ . Note that, unlike for the meson-exchange part, here the parameters entering the potential differ, reflecting the different quark masses and sizes of the  $K$  and  $\bar{D}$  mesons. As in the  $KN$  case, graphs (2) and (4) in Fig. 2 are suppressed as compared to graphs (1) and (3), because of the large quark mass in the denominator of Eq. (8). This suppression is even stronger in the  $\bar{D}N$  case. Note that graphs (1) and (3) actually become somewhat larger as compared to the kaon case because of the larger size of the  $D$  meson.

It is worth pointing out there are sizable effects due to the iteration of the interaction in the Lippmann-Schwinger equation. In order to demonstrate this we include also results obtained in Born approximation for the  $I = 1$  channel. These are shown by the dotted lines in Fig. 5. Obviously, close to threshold the Born result for the  $\bar{D}N$  cross section is of the order of 30 mb, while the corresponding unitarized result is of the order of 10 mb, i.e. there is more than 50 % difference.

Our full predictions for the  $\bar{D}N$  cross sections, combining now the mesonic part with the contributions from quark-gluon processes, are presented in Fig. 6. The solid lines are results for the scenario where the scalar-meson contributions are viewed as being due to correlated  $\pi\pi - K\bar{K}$  exchange, in line with the philosophy of the original Jülich  $KN$  model [12]. In this case the cross section for  $I = 1$  is in the order of 20 mb, i.e. roughly twice as large as observed for the  $KN$  system [29]. For the  $I = 0$  channel we predict a cross section that is practically zero at the threshold but increases to about 25 mb at the excess energy 150 MeV. Also here the result is roughly twice as large as the cross section for  $KN$  at the corresponding excess energy.

The dashed curves show results obtained in the scenario that attempts to simulate the case that the scalar contributions are due to genuine scalar-meson exchange. In order to get a rough estimate for that scenario we assume here, for simplicity reasons, that the couplings for  $\bar{D}N$  are the same as for  $KN$  for the two scalar mesons in question. A strict evaluation within the SU(4) scheme would involve several unknown quantities such as the singlet couplings and the mixing angles and is not feasible. In any case, our prescription is only meant to illustrate the ambiguity resulting from the unclear situation in the scalar sector. Evidently, the cross section for  $I = 0$  is rather insensitive to the treatment of the scalar mesons, at least within the scenarios considered here. Indeed, due to their isospin structure, the contributions of the  $\sigma$  and the  $a_0(980)$  mesons tend to cancel in this channel. On the other hand, the predicted  $I = 1$  cross section reduces by 50 % for the scenario based on larger scalar-meson cou-

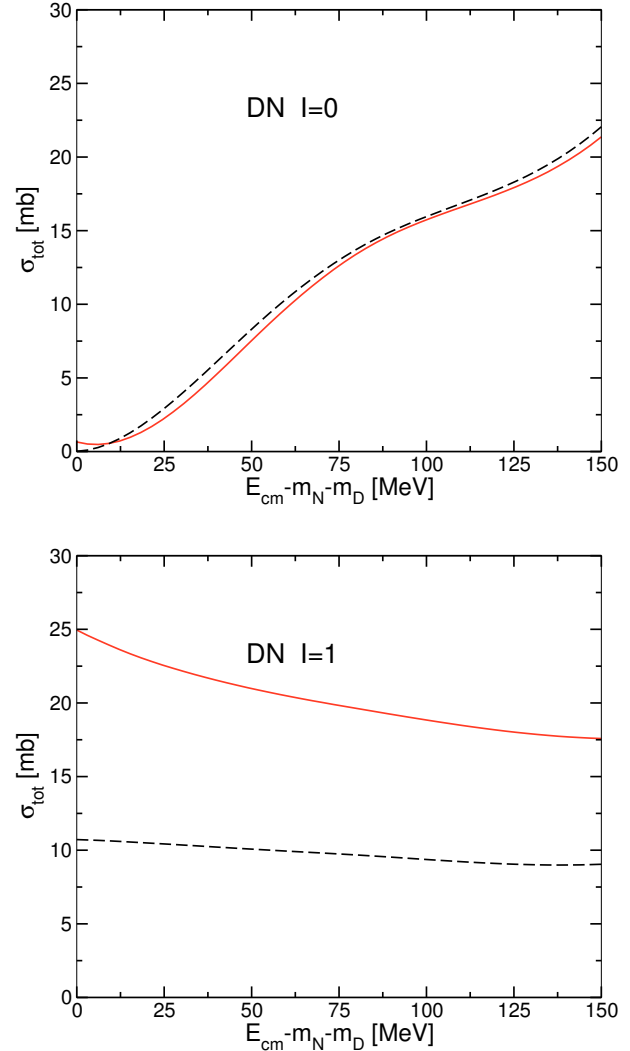


**Fig. 6.**  $\bar{D}N$  cross sections in the isospin channels  $I=0,1$ . The solid curves are the results of the full model, i.e. including meson-exchange and OGE, and viewing the scalar contributions to be due to correlated  $\pi\pi$  exchange. The dashed curves show results obtained in the scenario that attempts to simulate the case that the scalar contributions are due to genuine scalar-meson exchange, cf. text.

pling constants. This variation may be considered as a measure for the uncertainty in our model prediction for  $\bar{D}N$ , despite of constructing the interaction in close analogy to  $KN$  and invoking strict SU(4) symmetry.

Finally, for completeness let us also present the  $S$ -wave  $\bar{D}N$  phase shifts. Corresponding results are shown in Fig. 7, for the quark-gluon interaction alone (upper panel) and for the full model (lower panel). Obviously, in general all interactions are repulsive, as reflected in the negative sign of the phase shifts. But the full model is weakly attractive for energies near the threshold in the  $I = 0$  channel. The corresponding scattering lengths are  $a^{I=0} = -0.13$  fm,  $a^{I=1} = -0.29$  fm, for the quark-gluon interaction and  $a^{I=0} = 0.07$  fm,  $a^{I=1} = -0.45$  fm, for the full model. Interestingly, the former results are pretty close

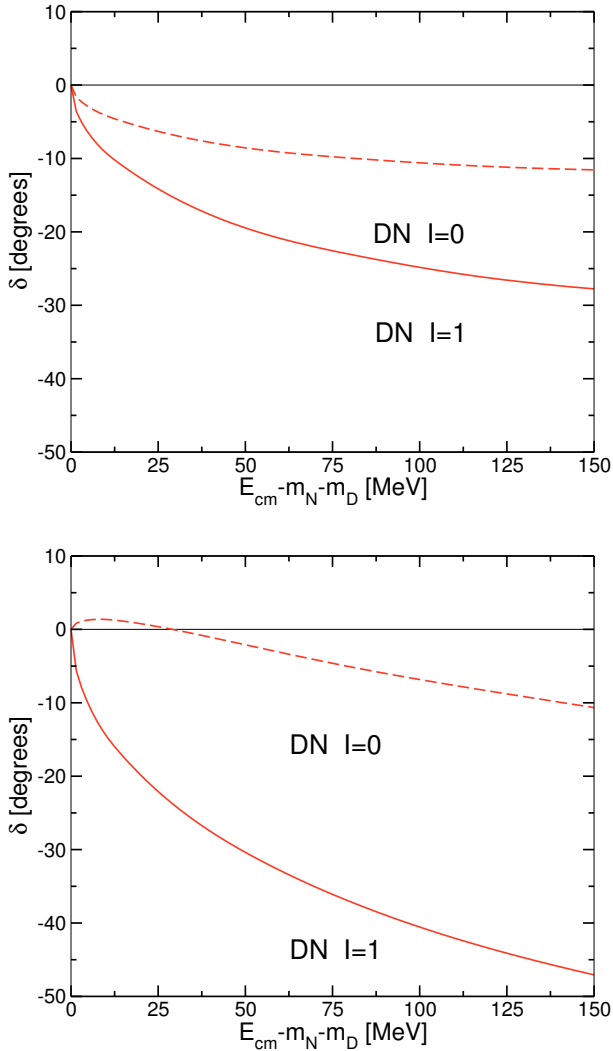


**Fig. 7.**  $\bar{D}N$   $S$ -wave phase shifts in the isospin channels  $I=0,1$ . The upper panel shows the results for the quark model based on OGE while the lower panel are the results of the full model, i.e. including meson-exchange and OGE, and viewing the scalar contributions to be due to correlated  $\pi\pi$  exchange.

to the values found by Lutz and Korpa for their  $\bar{D}N$  interaction [16] while the latter are qualitatively very similar to the results obtained for the  $KN$  interaction [12].

## 5 Summary

In this paper we presented predictions for the low-energy  $\bar{D}N$  cross section based on a model which was developed in close analogy to the meson-exchange  $KN$  interaction of the Jülich group [11, 12], utilizing  $SU(4)$  symmetry constraints. The main ingredients of the interaction are provided by vector meson ( $\rho$ ,  $\omega$ ) exchange but higher-order box diagrams involving  $\bar{D}^*N$ ,  $\bar{D}\Delta$ , and  $\bar{D}^*\Delta$  intermediate states, are taken into account too. Furthermore, in the spirit of a recent study of the  $KN$  system by us [10], the short range part is again assumed to receive additional contributions from genuine quark-gluon processes.

The cross sections for  $\bar{D}N$  predicted for excess energies up to 150 MeV are of the same order of magnitude as those for  $KN$  but with average values of around 20 mb roughly a factor two larger than for the latter system. There is an uncertainty in our prediction for the  $I = 1$  channel which is caused by the unknown  $SU(4)$  structure of the scalar-meson sector. Assuming that the contributions in the scalar sector are due to correlated  $\pi\pi$  exchange, in line with the Jülich  $KN$  model, we find that the scalar contributions influence the  $\bar{D}N$  cross sections only marginally. But a scenario where the effect of the exchange of genuine scalar mesons is simulated by assuming their coupling strengths to be the same as in the  $KN$  model leads to a 50 % reduction of the  $I = 1$  cross section.

Anyway, the most interesting finding of our study is certainly the important role played by the  $\omega$ -exchange contribution. Its interference pattern with the  $\rho$ -exchange, which is basically fixed by the assumed  $SU(4)$  symmetry, clearly determines the qualitative features of the  $\bar{D}N$  interaction – similar to what happens also for the  $KN$  system. As a consequence also the cross sections predicted for  $\bar{D}N$  show qualitatively very similar features to those known of  $KN$  scattering. On the other hand, predictions for  $\bar{D}N$  where only  $\rho$ -exchange was taken into account differ drastically and, in our opinion, should be regarded with caution in view of the results presented in this paper.

## Acknowledgements

This work was financially supported by the Deutsche Forschungsgemeinschaft (Project no. 444 BRA-113/14) and the Brazilian agencies CAPES, CNPq and FAPESP. This work was supported in part by the EU I3HP “Study of Strongly Interacting Matter” under contract number RII3-CT-2004-506078, by the DFG through funds provided to the SFB/TR 16 “Subnuclear Structure of Matter”, by the EU Contract No. MRTN-CT-2006-035482, “FLAVIANet” and by BMBF (grant 06BN411). A.S. acknowledges support by the JLab grant SURA-06-C0452 and the COSY FFE grant No. 41760632 (COSY-085).

## A The interaction Lagrangians

Here we list the specific interaction Lagrangians which are used to derive the meson-exchange  $\bar{D}N$  interaction. The baryon-baryon-meson couplings are given by

$$\begin{aligned}
\mathcal{L}_{NNS} &= g_{NNS} \bar{\Psi}_N(x) \Psi_N(x) \Phi_S(x), \\
\mathcal{L}_{NNP} &= g_{NNP} \bar{\Psi}_N(x) i \gamma^5 \Psi_N(x) \Phi_P(x), \\
\mathcal{L}_{NNV} &= g_{NNV} \bar{\Psi}_N(x) \gamma_\mu \Psi_N(x) \Phi_V^\mu(x) \\
&\quad + \frac{f_{NNV}}{4m_N} \bar{\Psi}_N(x) \sigma_{\mu\nu} \Psi_N(x) (\partial^\mu \Phi_V^\nu(x) - \partial^\nu \Phi_V^\mu(x)), \\
\mathcal{L}_{N\Delta P} &= \frac{f_{N\Delta P}}{m_P} \bar{\Psi}_{\Delta\mu}(x) \Psi_N(x) \partial^\mu \Phi_P(x) + H.c., \\
\mathcal{L}_{N\Delta V} &= \frac{f_{N\Delta V}}{m_V} i (\bar{\Psi}_{\Delta\mu}(x) \gamma^5 \gamma_\mu \Psi_N(x) \\
&\quad - \bar{\Psi}_N(x) \gamma^5 \gamma_\mu \Psi_{\Delta\mu}(x)) (\partial^\mu \Phi_V^\nu(x) - \partial^\nu \Phi_V^\mu(x)), \\
\mathcal{L}_{NYP} &= \frac{f_{NYP}}{m_P} (\bar{\Psi}_Y(x) \gamma^5 \gamma^\mu \Psi_N(x) \\
&\quad + \bar{\Psi}_N(x) \gamma^5 \gamma^\mu \Psi_Y(x)) \partial_\mu \Phi_P(x). \tag{11}
\end{aligned}$$

Here  $\Psi_N$ ,  $\Psi_{\Delta\mu}$ , and  $\Psi_Y$  are the nucleon,  $\Delta$ , and hyperon field operators and  $\Phi_S$ ,  $\Phi_P$ , and  $\Phi_V^\mu$  are the field operators for scalar, pseudoscalar and vector mesons, respectively.

The employed three-meson couplings are

$$\begin{aligned}
\mathcal{L}_{PPS} &= g_{PPS} m_P \Phi_P(x) \Phi_P(x) \Phi_S(x), \\
\mathcal{L}_{PPV} &= g_{PPV} \Phi_P(x) \partial_\mu \Phi_P(x) \Phi_V^\mu(x), \\
\mathcal{L}_{VVP} &= \frac{g_{VVP}}{m_V} i \epsilon_{\mu\nu\tau\delta} \partial^\mu \Phi_V^\nu(x) \partial^\tau \Phi_V^\delta(x) \Phi_P(x), \tag{12}
\end{aligned}$$

where  $\epsilon_{\mu\nu\tau\delta}$  is the antisymmetric tensor with  $\epsilon^{0123} = 1$ . Note that here only the space-spin part is given. The additional SU(4) flavour structure that leads to the characteristic relations between the coupling constants is discussed in Sect. II. Details on the derivation of the meson-baryon interaction potential from those Lagrangians can be found in Refs. [11, 12].

## B The quark-model meson-baryon interaction

In this Appendix we outline the derivation of the effective meson-baryon interaction in the quark model. As already mentioned, the effective interaction is given by the quark-Born diagrams depicted in Fig. 2. Their expressions can be obtained in the Born-order quark interchange model [33], or using the methods of the resonating group, or the Fock-Tani representation [34]. Given the interactions and the bound state amplitudes of the single hadrons, the expression of the quark Born diagrams for the effective meson-baryon interaction  $\alpha + \beta \rightarrow \gamma + \delta$  is given by

$$\begin{aligned}
\mathcal{V}_{MB}^{(\alpha\beta;\gamma\delta)} &= -3 \Phi_\gamma^{*\mu\nu_1} \Psi_\delta^{*\nu\mu_2\mu_3} V_{qq}(\mu\nu; \sigma\rho) \Phi_\alpha^{\rho\nu_1} \Psi_\beta^{\sigma\mu_2\mu_3} \\
&\quad - 3 \Phi_\gamma^{*\sigma\rho} \Psi_\delta^{*\mu_1\mu_2\mu_3} V_{q\bar{q}}(\mu\nu; \sigma\rho) \Phi_\alpha^{\mu_1\nu} \Psi_\beta^{\mu_2\mu_3} \\
&\quad - 6 \Phi_\gamma^{*\mu_1\nu_1} \Psi_\delta^{*\nu\mu_2\mu_3} V_{qq}(\mu\nu; \sigma\rho) \Phi_\alpha^{\rho\nu_1} \Psi_\beta^{\mu_1\sigma\mu_3} \\
&\quad - 6 \Phi_\gamma^{*\mu_1\nu} \Psi_\delta^{*\nu_1\mu_2\mu_3} V_{q\bar{q}}(\mu\nu; \sigma\rho) \Phi_\alpha^{\nu_1\rho} \Psi_\beta^{\mu_1\sigma\mu_3}. \tag{13}
\end{aligned}$$

Here, the  $\Phi$  and  $\Psi$  are Fock-space amplitudes of the one-meson and one-baryon states, which in a second quantization notation are given as

$$|M_\alpha\rangle = \Phi_\alpha^{\mu\nu} q_\mu^\dagger \bar{q}_\nu^\dagger |0\rangle, \quad |B_\alpha\rangle = \frac{1}{\sqrt{3!}} \Psi_\alpha^{\mu_1\mu_2\mu_3} q_{\mu_1}^\dagger q_{\mu_2}^\dagger q_{\mu_3}^\dagger |0\rangle, \tag{14}$$

where  $\alpha$  indicates all quantum numbers necessary to specify the hadronic state, like c.m. momentum, spin and flavor, and  $\mu, \nu, \dots$  indicate all quantum numbers of the quarks like momentum, color, spin and flavor – a sum or integral over repeated indices is implied.  $q^\dagger$ ,  $\bar{q}^\dagger$ ,  $q^\dagger$ , and  $\bar{q}$  are quark and antiquark creation and annihilation operators that satisfy the usual canonical anticommutation relations. In addition,  $V_{qq}$ ,  $V_{\bar{q}q}$  and  $V_{q\bar{q}}$  are the microscopic quark and antiquark interactions, which in the same second quantization notation are defined through

$$\begin{aligned}
V &= \frac{1}{2} V_{qq}(\mu\nu; \rho\sigma) q_\mu^\dagger q_\nu^\dagger q_\sigma q_\rho + \frac{1}{2} V_{\bar{q}\bar{q}}(\mu\nu; \rho\sigma) \bar{q}_\mu^\dagger \bar{q}_\nu^\dagger \bar{q}_\sigma \bar{q}_\rho \\
&\quad + V_{q\bar{q}}(\mu\nu; \rho\sigma) q_\mu^\dagger \bar{q}_\nu^\dagger \bar{q}_\sigma q_\rho^\dagger. \tag{15}
\end{aligned}$$

The expression for  $\mathcal{V}_{MB}$  in Eq. (13) involves a 6-dimensional integral that cannot be integrated analytically for general forms of the amplitudes  $\Phi$  and  $\Psi$ . However, when using Gaussian forms for the meson and baryon amplitudes, many of the integrals can be done analytically and the resulting expression for each of the diagrams of Fig. 2 is of the form given in Eq. (10). Specifically, we use for the amplitudes  $\Phi$  and  $\Psi$  in momentum space Gaussian forms with width parameters  $\beta_D$  and  $\alpha_N$  as

$$\Phi_P(\mathbf{k}_1, \mathbf{k}_2) = \delta^{(3)}(\mathbf{P} - \mathbf{k}_1 - \mathbf{k}_2) \left( \frac{1}{\pi\beta_D^2} \right)^{3/2} e^{-\mathbf{k}_{rel}^2/8\beta_D^2}, \tag{16}$$

where

$$\mathbf{k}_{rel} = \frac{2(M_q \mathbf{k}_1 - M_{\bar{q}} \mathbf{k}_2)}{M_q + M_{\bar{q}}}, \tag{17}$$

and

$$\begin{aligned}
\Psi_P(\mathbf{k}_1, \mathbf{k}_2, \mathbf{k}_3) &= \delta^{(3)}\left(\mathbf{P} - \sum_{i=1}^3 \mathbf{k}_i\right) \left( \frac{3}{\pi^2 \alpha_N^4} \right)^{3/4} \\
&\quad \times e^{-\sum_{i=1}^3 (\mathbf{k}_i - \mathbf{P}/3)^2 / 2\alpha_N^2}. \tag{18}
\end{aligned}$$

Writing

$$V_{qq}(\mu\nu; \sigma\rho) = \delta(\mathbf{k}_\mu + \mathbf{k}_\nu - \mathbf{k}_\sigma - \mathbf{k}_\rho) v(\mathbf{k}_\mu - \mathbf{k}_\rho), \tag{19}$$

and equivalently for  $V_{q\bar{q}}$  and  $V_{\bar{q}\bar{q}}$ , after integrating over the quark momenta as indicated in Eq. (13) one obtains the expression given in Eq. (10), where the  $a_i, b_i, \dots$ , can be written as a ratio  $a_i = n(a_i)/d(a_i)\alpha_N^2$ ,  $b_i = n(b_i)/d(b_i)\alpha_N^2$ , etc. The corresponding expressions are given as follows:

Graph (1):

$$\begin{aligned}
n(a_1) &= 3g^2 + 3(1 + \rho)^2 + g(7 + 8\rho + 10\rho^2) \\
d(a_1) &= 6(3 + 2g)(1 + \rho)^2 \\
n(c_1) &= g^2 + (1 + \rho)^2 - 2g(-1 + \rho^2) \\
d(c_1) &= (3 + 2g)(1 + \rho)^2 \\
n(d_1) &= 3g, \quad d(a_1) = (3 + 2g) \\
n(e_1) &= -g(1 + 4\rho)(\mathbf{p} + \mathbf{p}') \\
d(e_1) &= (3 + 2g)(1 + \rho),
\end{aligned} \tag{20}$$

Graph (2):

$$\begin{aligned}
n(a_2) &= n(a_1), \quad d(a_2) = d(a_1) \\
n(b_2) &= n(b_1), \quad d(b_2) = d(b_1) \\
n(c_2) &= n(c_1), \quad d(c_2) = d(c_1) \\
n(d_2) &= g(3 + g), \quad d(d_2) = 2(3 + 2g) \\
n(e_2) &= g[(2 + g + 2\rho)\mathbf{p} - (1 + g - 2\rho)\mathbf{p}'] \\
d(e_2) &= (3 + 2g)(1 + \rho),
\end{aligned} \tag{21}$$

Graph (3):

$$\begin{aligned}
n(a_3) &= 3g^2 + 3(1 + \rho)^2 + g(7 + 8\rho + 10\rho^2) \\
d(a_3) &= 6(3 + 2g)(1 + \rho)^2 \\
n(b_3) &= n(a_3), \quad d(b_3) = d(a_3) \\
n(c_3) &= n(c_1), \quad d(c_3) = d(c_1) \\
n(d_3) &= 6 + 7g, \quad d(d_3) = 4(3 + 2g) \\
n(e_3) &= -3[1 + g + (1 + 2g)\rho]\mathbf{p} + [3 + g + (3 - 2g)\rho]\mathbf{p}' \\
d(e_3) &= 2(3 + 2g)(1 + \rho),
\end{aligned} \tag{22}$$

Graph (4):

$$\begin{aligned}
n(a_4) &= n(a_1), \quad n(b_4) = n(b_1) \\
d(a_4) &= d(a_1), \quad d(b_4) = d(b_1) \\
n(c_4) &= n(c_1), \quad d(c_4) = d(c_1) \\
n(d_4) &= 2 + g, \quad d(d_4) = 4 \\
n(e_4) &= -(1 + g + \rho)(\mathbf{p} - \mathbf{p}') \\
d(e_4) &= 2(1 + \rho).
\end{aligned} \tag{23}$$

In these,  $g = \alpha_N^2/\beta_D^2$  and  $\rho = M_u/M_c$ .

## References

1. T. Matsui and H. Satz, Phys. Lett. B **178**, 416 (1986).
2. R. L. Thews, M. Schroedter and J. Rafelski, Phys. Rev. C **63**, 054905 (2001) [arXiv:hep-ph/0007323].
3. H. Satz, J. Phys. G **32**, R25 (2006) [arXiv:hep-ph/0512217].
4. M. Kotulla et al., *Technical Progress Report for  $\bar{P}$ ANDA, Strong Interaction Studies with Antiprotons*, February 2005, [http://www.panda.gsi.de/db/papersDB/PC19-050217\\_panda\\_tpr.pdf](http://www.panda.gsi.de/db/papersDB/PC19-050217_panda_tpr.pdf).
5. W. Cassing, Y. S. Golubeva and L. A. Kondratyuk, Eur. Phys. J. A **7**, 279 (2000) [arXiv:nucl-th/9911026].
6. T. Barnes, arXiv:nucl-th/0306031.
7. Z. w. Lin, C. M. Ko and B. Zhang, Phys. Rev. C **61**, 024904 (2000) [arXiv:nucl-th/9905003].
8. A. Sibirtsev, K. Tsushima and A. W. Thomas, Eur. Phys. J. A **6**, 351 (1999) [arXiv:nucl-th/9904016].
9. A. Sibirtsev, Nucl. Phys. A **680**, 274c (2001).
10. D. Hadjimichef, J. Haidenbauer and G. Krein, Phys. Rev. C **66**, 055214 (2002) [arXiv:nucl-th/0209026].
11. R. Büttgen, K. Holinde, A. Müller–Groeling, J. Speth, and P. Wyborny, Nucl. Phys. **A506**, 586 (1990).
12. M. Hoffmann, J.W. Durso, K. Holinde, B.C. Pearce, and J. Speth, Nucl. Phys. **A593**, 341 (1995).
13. J. Haidenbauer and G. Krein, Phys. Rev. C **68**, 052201 (2003) [arXiv:hep-ph/0309243].
14. J. Hofmann and M. F. M. Lutz, Nucl. Phys. A **763**, 90 (2005) [arXiv:hep-ph/0507071].
15. L. Tolos, J. Schaffner-Bielich and A. Mishra, Phys. Rev. C **70**, 025203 (2004) [arXiv:nucl-th/0404064].
16. M. F. M. Lutz and C. L. Korpa, Phys. Lett. B **633**, 43 (2006) [arXiv:nucl-th/0510006].
17. T. Mizutani and A. Ramos, Phys. Rev. C **74**, 065201 (2006) [arXiv:hep-ph/0607257].
18. R. Machleidt, K. Holinde, Ch. Elster, Phys. Rep. **149**, 1 (1987).
19. S.G. Matinyan and B. Müller, Phys. Rev. C **58**, 2994 (1998). Note that the actual coupling constant given in that reference is a factor of 2 larger due to the difference of the definitions.
20. Z.-w. Lin and C. M. Ko, Phys. Rev. C **62**, 034903 (2000) [arXiv:nucl-th/9912046].
21. Z.-w. Lin, T. G. Di and C. M. Ko, Nucl. Phys. A **689**, 965 (2001) [arXiv:nucl-th/0006086].
22. W. Liu and C. M. Ko, Phys. Lett. B **533**, 259 (2002) [arXiv:nucl-th/0201074].
23. E. Klempt, arXiv:hep-ph/0404270.
24. Y. Kalashnikova, A. E. Kudryavtsev, A. V. Nefediev, J. Haidenbauer, and C. Hanhart, Phys. Rev. C **73**, 045203 (2006) [arXiv:nucl-th/0512028].
25. J. Haidenbauer and U.-G. Meißner, Phys. Rev. C **72**, 044005 (2005) [arXiv:nucl-th/0506019].
26. P. Kroll, B. Quadder and W. Schweiger, Nucl. Phys. B **316**, 373 (1989).
27. A. B. Kaidalov and P. E. Volkovitsky, Z. Phys. C **63**, 517 (1994).
28. A. Müller–Groeling, K. Holinde, and J. Speth, Nucl. Phys. **A513**, 557 (1990).
29. A. Sibirtsev, J. Haidenbauer, S. Krewald and U.-G. Meißner, J. Phys. G **32**, R395 (2006) [arXiv:nucl-th/0608028].
30. T. Barnes and E. S. Swanson, Phys. Rev. C **49**, 1166 (1994).
31. K. Martins, D. Blaschke and E. Quack, Phys. Rev. C **51**, 2723 (1995) [arXiv:hep-ph/9411302].
32. J. P. Hilbert, N. Black, T. Barnes and E. S. Swanson, arXiv:nucl-th/0701087.
33. T. Barnes, E. S. Swanson and J. D. Weinstein, Phys. Rev. D **46**, 4868 (1992) [arXiv:hep-ph/9207251].
34. D. Hadjimichef, G. Krein, S. Szpigel and J. S. da Veiga, Annals Phys. **268**, 105 (1998) [arXiv:hep-ph/9805459].